Stick-slip friction and wear of articular joints

Dong Woog Lee[a], Xavier Banquy[a], and Jacob N. Israelachvili[a,b,1]

[a]Department of Chemical Engineering and [b]Materials, University of California, Santa Barbara, CA 93106

Contributed by Jacob N. Israelachvili, December 26, 2012 (sent for review October 19, 2012)

Stick-slip friction was observed in articular cartilage under certain loading and sliding conditions and systematically studied. Using the Surface Forces Apparatus, we show that stick-slip friction can induce permanent morphological changes (a change in the roughness indicative of wear/damage) in cartilage surfaces, even under mild loading and sliding conditions. The different load and speed regimes can be represented by friction maps—separating regimes of smooth and stick-slip sliding; damage generally occurs within the stick-slip regimes. Prolonged exposure of cartilage surfaces to stick-slip sliding resulted in a significant increase of surface roughness, indicative of severe morphological changes of the cartilage superficial zone. To further investigate the factors that are conducive to stick-slip and wear, we selectively digested essential components of cartilage: type II collagen, hyaluronic acid (HA), and glycosaminoglycans (GAGs). Compared with the normal cartilage, HA and GAG digestions modified the stick-slip behavior and increased surface roughness (wear) during sliding, whereas collagen digestion decreased the surface roughness. Importantly, friction forces increased up to 2, 10, and 5 times after HA, GAGs, and collagen digestion, respectively. Also, each digestion altered the friction map in different ways. Our results show that (*i*) wear is not directly related to the friction coefficient but (*ii*) more directly related to stick-slip sliding, even when present at small amplitudes, and that (*iii*) the different molecular components of joints work synergistically to prevent wear. Our results also suggest potential noninvasive diagnostic tools for sensing stick-slip in joints.

arthritis | biolubrication | biointerface | boundary lubrication

Osteoarthritis (OA) is widely present in the elderly (1, 2) as well as people with obesity (3). Despite the prevalence of OA, the physical and biological events that trigger articular cartilage damage are still poorly understood, especially at the molecular and submicron levels; so far, no model has been successful in describing the mechanistic cascade that leads to cartilage wear and irreversible loss (4). There are no available techniques to detect the onset of joint diseases, and tracking the progression of these diseases remains a major challenge (5).

One of the key challenges for establishing a model that can successfully track the cause and progression of joint diseases is in the fact that articular joints are designed to function under an extremely large range of mechanical, dynamic, and environmental conditions, under any of which a priori damage can occur. Many scientists have, therefore, focused their efforts on specific physiological regimes under which joints would be severely subjected to mechanical damage caused by a failure of the lubrication mechanism at the submicron level.

The most important and also least understood physiological regime associated with damage is referred to as the boundary lubrication (BL) regime, where two sliding surfaces and the molecular species that are attached to them are in intimate contact during most of the motion. It is now well-known that, in the BL regime, wear of soft surfaces, especially cartilage, can easily and quickly propagate as long as the surfaces are subjected to a high enough normal load (typically above several Newtons corresponding to normal pressures ranging from 1 to 10 MPa) and sliding speeds (typically above millimeters per second) (6). Under these conditions, the rheological (viscous) properties of the lubricating fluid do not contribute significantly to the lubrication of the surfaces, and it is the macromolecules that are present in the interstitial gap separating the surfaces that lubricate and ultimately, protect the surfaces from wear. Boundary lubrication can be achieved in many ways and is not limited to high loads or prolonged sliding; it can also be achieved under mild loading conditions (typically by applying a load in the range of several milliNewtons corresponding to a normal pressure of ~0.1 MPa) as long as the sliding speed is low enough (or zero under quasistatic conditions such as sitting or standing) to avoid elastohydrodynamic deformations of the surfaces and the development of a thick lubricating fluid between the surfaces. Wear of articular surfaces has never been studied under such mild conditions, and therefore, no mechanism has been proposed to describe its occurrence.

In this study, we show that, under mild sliding conditions corresponding to conditions of a human being at rest, stable intermittent sliding between two articular surfaces can be observed. Together with stiction spike (7, 8), stick-slip sliding is commonly at the origin of irreversible transformations of surfaces and in this study, cartilage topography—a hallmark of all cartilage wear processes. By selectively digesting specific components [collagen, hyaluronic acid (HA), and glycosaminoglycans (GAGs)] of the cartilage surfaces, we aimed to establish correlations between structural changes of joint components and their subsequent impact on the frictional map of the articular joint as they occur during OA.

Many different experimental setups have been proposed for measuring frictional forces between cartilage surfaces (9–12). Most of these setups can be schematically represented by a mechanical equivalent depicted in Fig. 1*A*. When characterizing complex frictional behaviors like stick-slip, one can readily see that the measured average friction force is not the only important or even the most important parameter defining the system when intermittent friction is present (including other transient effects, such as stiction). The inertia of the moving parts, the system resonance frequencies, the mass (m), and the stiffness (K) are also key experimental parameters.

Significance

The goal of this study was to use the Surface Forces Apparatus to examine the effects of slip-stick friction on cartilage surface morphology under different loading and sliding conditions. Different load and speed regimes were represented using friction maps that separated regimes of smooth and stick-slip sliding. The finding of this work is that damage generally occurs within the stick-slip regimes and is not directly related to the friction coefficient. Prolonged exposure of cartilage surfaces to stick-slip sliding resulted in a significant increase of surface roughness, indicative of severe morphological changes (damage) of the cartilage surfaces.

Author contributions: D.W.L., X.B., and J.N.I. designed research; D.W.L. and X.B. performed research; D.W.L. analyzed data; and D.W.L., X.B., and J.N.I. wrote the paper.

The authors declare no conflict of interest.

Freely available online through the PNAS open access option.

[1]To whom correspondence should be addressed. E-mail: jacob@engineering.ucsb.edu.

This article contains supporting information online at www.pnas.org/lookup/suppl/doi:10.1073/pnas.1222470110/-/DCSupplemental.

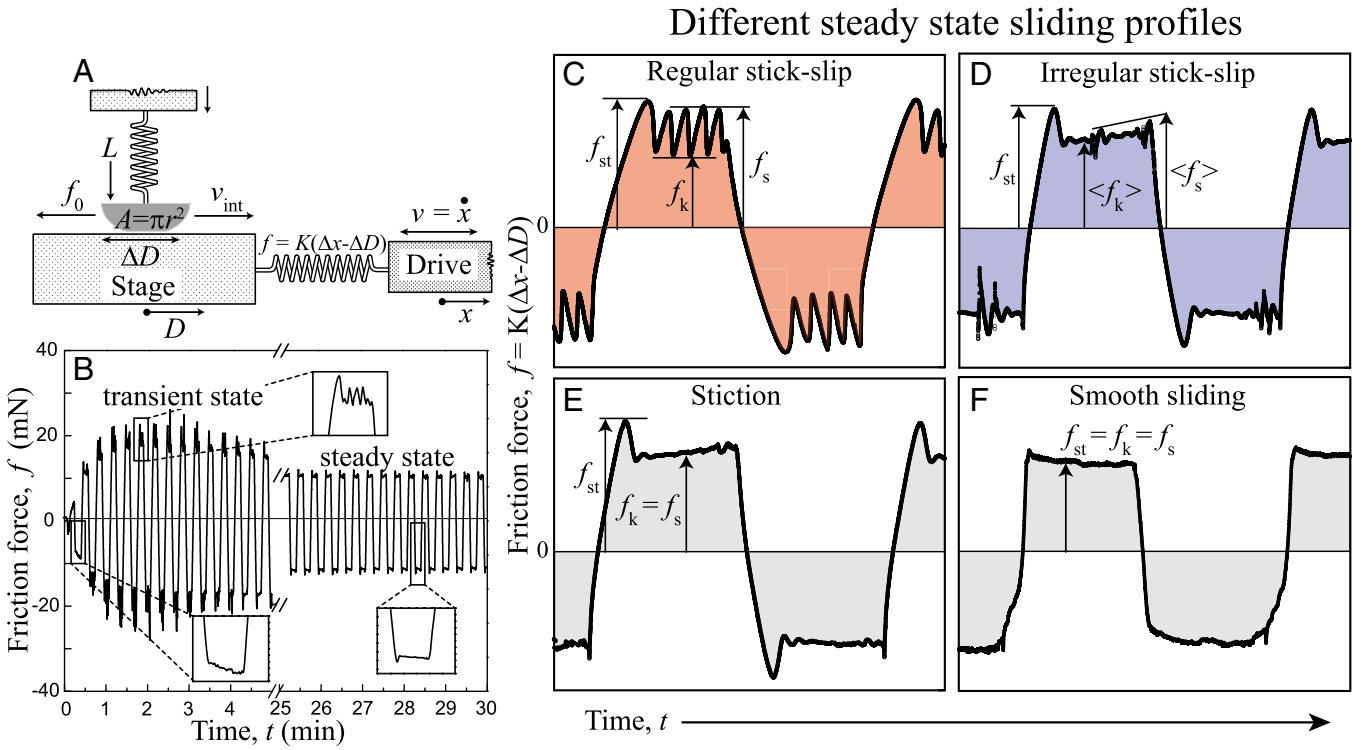

Fig. 1. (*A*) Schematic of the principle of SFA used for measuring normal load, *L*, and friction force, *f*, between two surfaces in contact with area *A* under back and forth shearing motion of peak-to-peak amplitude *D* ~100 μm and driving velocity, *v*. The friction force, *f*, is measured as $f = K(\Delta x - \Delta D)$, where Δx and ΔD are the displacement of the drive and the stage, respectively, and *K* is the stiffness of the measuring spring. (*B*) Evolution of friction forces with time measured between two cartilage surfaces in synovial fluid at a driving speed of *v* = 10 μm/s. Right after loading and applying shear motion, the friction force increases rapidly and evolves to stick-slip or irregular stick-slip sliding motion (*B Insets*). After sliding for 3 min, the friction force gradually decreases to a steady-state value, and sliding phase becomes smooth. Four distinct sliding behaviors are observed depending on the sliding conditions: (*C*) regular stick-slip, (*D*) irregular stick-slip, (*E*) smooth sliding with stiction, and (*F*) purely smooth sliding.

As can be seen in Fig. 1*A*, the applied force *f* by the spring coupling the drive to the stage and the speed *v* of the drive are different from the true interfacial friction force, f_0, and sliding speed, v_{int}. Starting from rest, the stage will move when the applied force *f* reaches the friction force, f_0. If the static friction (also known as the stiction) force, f_{st}, is greater than the kinetic friction force, f_k (Fig. 1*C*), the stage will accelerate rapidly to a speed, v_{int}, much greater than the slider speed, *v*, and the coupling spring will be compressed. At this point, the stage will decelerate to a stop, where the friction force recovers to its high value, f_{st}. This cycle, called stick-slip, can be repeated periodically as long as the driver moves at a constant velocity.

Different models have been developed that aim to establish how macroscopic system properties and nanoscopic (i.e., molecular ordering) properties cooperate to create complex frictional motions like stick-slip. For a review of the different mechanisms of stick-slip, the reader is referred to refs. 13 and 14. Our experiments show that the stick-slip motion of cartilage surfaces is clearly velocity-dependent and restricted to a velocity window that depends on the applied normal load, *L*. In general, velocity windows for stick-slip are determined by two critical velocities (15): the first velocity, v_c^I, corresponds to the appearance of stick-slip and the onset of the velocity weakening regime of the friction force, f_0. The second velocity, v_c^{II}, corresponds to the disappearance of stick-slip, at which point $f = f_k$ = constant. In between v_c^I and v_c^{II}, different types of stick-slip motions can be observed, ranging from regular stick-slip (Fig. 1*A*) to irregular stick-slip (both in amplitude and frequencies, and stiction (Fig. 1 *D* and *E*). The determination of v_c^I and v_c^{II} as a function of the applied load allows a friction map to be established that characterizes the frictional behavior of a system.

Results and Discussion

A series of friction force measurements with cartilage against cartilage (Fig. 2*A*) were performed over a wide range of driving speeds (0.03–100 μm/s) and loads (5–250 mN) (details in *Materials and Methods*). Morphological studies were also performed by monitoring the cartilage surfaces before and after sliding using interferometry. Additionally, cartilage surfaces were treated with specific enzymes to investigate the effects of essential components on different friction and lubrication properties. The essential components of articular cartilage that we selected to digest are HA, GAGs, and type II collagen. All three components exhibit different and important roles in cartilage lubrication and malfunction: modification or digestion of each component is known to be highly related to the onset and progression of OA (11, 16–21).

Normal (Untreated) Cartilage. Fig. 2*A* shows a schematic of the friction experiments performed with normal (untreated) cartilage. Two opposing cartilage surfaces were sheared at a reciprocal motion of peak-to-peak amplitude ΔD (~100 μm) and back and forth driving velocity $\pm v$ under the applied load *L*. The Surface Forces Apparatus (SFA) chamber was saturated with water vapor to prevent the evaporation of the liquid droplet between two cartilage surfaces during the experiments. [Two hundred microliters equine synovial fluid (Fig. 2 *C* and *D*) or PBS buffer solution (all other experiments) were used. Friction phase diagrams show similar trends regardless of the type of fluid between two cartilage surfaces.] Fig. 2*B* shows the effect of *L* and *v* on f_k, and two distinct lubrication regimes can be clearly seen: (*i*) Fluid Film Lubrication (FFL; $0 < L < 10$ mN, $P \sim 0.07$ MPa) with a low friction coefficient ($\mu = \partial f_k/\partial L = 0.01$–$0.02$) and (*ii*)

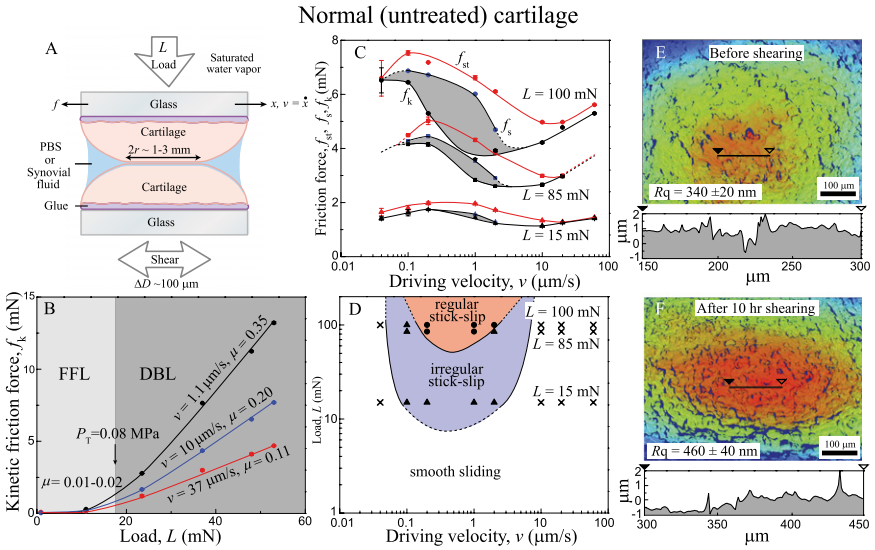

Fig. 2. (*A*) Schematic of the experimental setup used with measured and calculated variables. (*B*) Kinetic friction force (f_k) vs. load (L) curve under different driving velocities (v = 1.1, 10, and 37 μm/s) showing low-friction coefficient (μ = 0.01–0.2) in the FFL regime (L < 16 mN) and high-friction coefficient (μ = 0.11–0.35) in the DBL regime (L > 16 mN). (*C*) Friction forces (f_{st}, f_s, and f_k) vs. driving velocity (v) curve measured at three different loads (L = 100, 85, and 15 mN). The shaded regions indicate the stick-slip sliding regime. (*D*) Friction map showing representation of cartilage lubrication profiles. The dotted lines indicate the observed and measured trends based on the experiments and theories (15). (*E* and *F*) Topographic images (top view) of the contact zone of normal (nondigested) cartilage (*E*) before and (*F*) after 10 h shearing in stick-slip conditions. Red and blue colors indicate higher and lower heights, respectively. Single height profiles are also shown below each image.

Diffuse (Osmotic) BL (DBL; L > 25 mN, P ~ 0.09 MPa) with a much higher friction coefficient (μ = 0.11–0.35) (Fig. S1 shows a conventional Stribeck curve). [This regime is likely the same as the "Osmotic Lubrication" or "Brush Border Lubrication" regimes previously proposed by McCutchen (22, 23).] The transition load, L_T, where the lubrication mechanism changes from FFL to DBL is L_T ~ 16 mN/m (P ~ 0.08 MPa), which is similar to the value measured by Greene et al. (9) (Eq. S1 shows the pressure calculation). Additional insights into how v and L influence friction forces (of normal cartilage) and steady-state sliding profiles (Fig. 2 *C* and *D*) were gained by systematically changing v and L over a wide range of conditions (0.03–60 μm/s and 15–100 mN, respectively).

Fig. 2*C* shows how the friction forces (f_{st}, f_s, and f_k) change with v at three different loads (L = 15, 85, and 100 mN), and Fig. 2*D* shows the corresponding friction map. At L = 100 mN, stick-slip was observed at v_c^I = 0.03 μm/s. As v increases, the magnitude of the stick-slip spikes, $\Delta f = f_s - f_k$, increases until v = 1 μm/s; f_s then decreases until the driving speed reaches $v = v_c^{II}$ ~ 5 μm/s, where the stick-slip sliding disappears ($f_s = f_k$). As the load decreases, v_c^I increases, whereas v_c^{II} decreases, moving all of the values closer. Accordingly, the velocity window of stick-slip regime decreases, and by L = 15 mN, the stick-slip window becomes very narrow, with only irregular stick-slip being observed.

The friction map (Fig. 2*D*) conveniently illustrates the different stick-slip and smooth sliding regimes or windows as a function of L and v—two variables that can easily be controlled. Such maps can be used to determine and avoid the critical conditions that lead to stick-slip and abrasive wear not only in cartilage but also, many other lubricating systems.

Detailed studies of how shearing alters the morphology of normal articular cartilage were carried out by interferometric imaging because of the ability to scan areas and fast acquisition times, which has been used to image cartilage surfaces (24) (*Materials and Methods*). Approximately 1-μm-high and approximately 1-μm-deep valleys were observed on normal cartilage surfaces with an rms height roughness of Rq = 340 ± 20 nm. When sheared for 1.5 h (1 h under stick-slip sliding and 0.5 h under smooth sliding conditions), there was no change in the roughness. However, after sheared for ~10 h under stick-slip conditions, a significant and systematic increase in the roughness (Rq → 460 ± 40 nm) was observed, whereas no morphological change was observed under ~10 h shearing under smooth sliding conditions (Fig. S2). These results imply that, even under mild loading and sliding conditions, healthy cartilage can suffer irreversible damage but only under prolonged stick-slip sliding conditions.

HA-Digested Cartilage. HA is an anionic polysaccharide that is widely distributed in the human body and especially prevalent in articular joints. Because of its high molecular mass (3–4 MDa), HA has long been considered to be one of the major (bulk or boundary) lubricants that lowers the friction coefficient and protects cartilage surfaces from damage (25). Recent studies showed that physisorbed HA layers do not have a beneficial effect on lubrication, whereas chemically grafted and/or cross-linked HA layers exhibit excellent wear protection against surfaces, even when sheared at high pressures (~20 MPa), regardless of the high friction coefficient of μ = 0.15–0.3 (26, 27). Experiments involving selective digestion of HA from articular cartilage have shown that HA is mechanically trapped at the cartilage interface by the constricted collagen pore network (9) and that digestion of HA induces a decrease in the porosity and an increase in the stiffness of articular cartilage (10). The molecular mass of the HA is known to decrease (from ~3–4 down to 0.5 MDa) with age (18) and/or the progression of arthritis (16, 17).

Fig. 3 shows the effects of enzymatic digestion of HA on the friction forces, friction profiles, and topography of the cartilage surfaces before and after digestion and shearing. Compared with normal, healthy cartilage (Fig. 3 *A* and *B*), HA-digested cartilage (Fig. 3 *C*–*F*) exhibits noticeably different friction characteristics and topography: (*i*) a higher friction force (up to two times) (Fig. 3*C*), (*ii*) a decrease in the second critical velocity and a left upward shift of the friction map (Fig. 3*D*), and (*iii*) significant roughening of the cartilage surface (up to 25%) after 1.5 h of

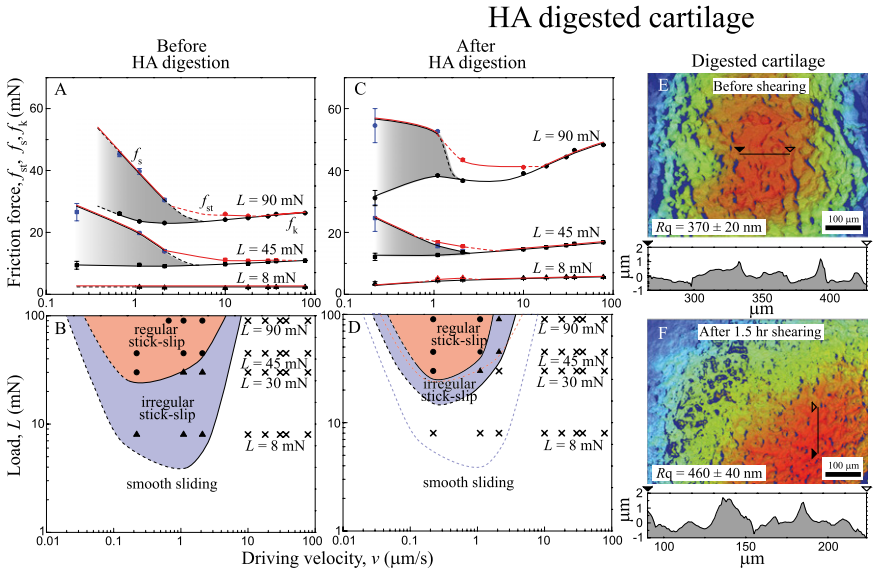

Fig. 3. (*A* and *C*) Friction forces vs. sliding velocity curve and (*B* and *D*) friction maps (*A* and *B*) before and (*C* and *D*) after HA digestion. (*E* and *F*) 3D images (top view) of HA-digested cartilage (*E*) before and (*F*) after 1.5 h shearing (1 h stick-slip and 0.5 h smooth sliding conditions).

shearing (1 h under stick-slip sliding and 0.5 h on smooth sliding conditions) (Fig. 3 *E* and *F*).

The *R*q value of HA-digested cartilages increased from 370 ± 20 to 460 ± 40 nm after 1.5 h of shearing (1 h under stick-slip sliding and 0.5 h under smooth sliding), which is similar to the increase in *R*q of normal cartilage sheared under stick-slip conditions for 10 h. Significant roughening of the shearing surfaces could be another reason for the observed increase in the friction force, although there seems to be no simple or direct correlation between the roughness and the friction force (28, 29) for soft surfaces like cartilage.

These results show that, at relatively high loads ($L > 45$ mN, $P > 0.11$ MPa), the main function of HA is to act as a surface-anchored protective layer rather than a bulk viscosity lubricant (9). To act as a well-functioning protective layer, HA should have a high enough molecular mass to both be trapped in the porous structure of the cartilage and entangle lubricin (LUB) for efficient boundary lubrication (9, 10). After digestion, the length of the HA chains is greatly shortened, and they lose the ability to become trapped in the porous structure of the cartilage. This increase in HA chains mobility causes the LUB and HA to be pushed out of the shearing contact under high L and v, leading to an increase in the friction force by a factor of approximately two and changing the stick-slip characteristics.

GAGs-Digested Cartilage. GAGs are known to have a high affinity for HA, forming large multimolecular aggregates. Such aggregates are highly sulfated, forming a large anion immobilized in the porous collagen network. This entropically confined GAGs–HA complex increases the osmotic pressure within the network, causing interstitial fluid pressurization and giving rise to improved load-bearing properties and compressive stiffness of the cartilage (12, 30). Highly hydrated GAGs are also known to enhance the hydration repulsion between two surfaces, which decreases the friction coefficient (12, 31–33).

In the early stages of OA, aggrecanases are found to be overexpressed and prevent the formation of GAGs–HA complex by cleaving the G1 domain, which contains the HA binding region (19). When GAGs lose their binding affinity to HA, GAGs rapidly diffuse out of the cartilage matrix. The decrease in GAGs concentration causes a loss in the ability of the cartilage to induce an osmotic pressure balance within cartilage matrix and increases its vulnerability to loading and shearing (30). Here, we used Chondroitinase ABC (Case ABC), which destroys mostly the chondroitin sulfate (34) and therefore, has similar effects to the cartilage as aggrecanase.

Fig. 4 shows the effects of enzymatic digestion of GAGs on the friction forces, friction profiles, and topography of cartilage surfaces before (Fig. 4 *A* and *B*) and after (Fig. 4 *C*–*F*) Case ABC treatment. Compared with normal cartilage, cartilage treated with Case ABC shows different friction characteristics and topography, highlighted as (*i*) higher friction force (up to 10 times) (Fig. 4*C*), (*ii*) increase in v_c^{II} and right downward shift of the friction map (Fig. 4*D*), and (*iii*) slight roughening of the cartilage surface (up to 10%) after 1.5 h of shearing. It is noteworthy that, although the increase in roughness was much less compared with HA-digested cartilage, the friction force increase was significantly higher.

The failure to maintain an osmotic balance within the cartilage and preserve the hydration layer at the interface explains the significant increase in the friction force after GAGs digestion. Furthermore, interpenetration and entanglements of HA chains between opposing surfaces is facilitated because of the absence of GAGs, further leading to higher friction forces (35). Regardless, the protective HA layer is still intact at the interfaces, which minimizes morphological changes compared with HA-digested cartilage.

Collagen-Digested Cartilage. Type II collagen occupies 60–80% of the solid fraction of cartilage to form a porous fibril network (12, 36–39) that governs the mechanical properties, deformation response, and friction of cartilage (30, 40). The disruption of the fibril network and softening of cartilage have been observed at the onset and progression of OA (20, 21), which could also be induced by applying type II collagenase (41, 42). Recent studies (10) indicate that enzymatic digestion of collagen causes drastic disruption of the complex microstructure and stability of the pore matrix, jeopardizing the cartilage's ability to control the transport of interstitial fluid through diffusion and/or flow, and inhibits efficient hydrodynamic lubrication.

Fig. 5 shows the effect of type II collagen digestion on the friction force, friction profiles, and topography of the sheared cartilage surfaces. Compared with normal cartilage (Fig. 4 *A* and *B*), collagen-digested cartilage (Fig. 4 *C*–*F*) shows different friction characteristics and topography, such as (*i*) higher friction

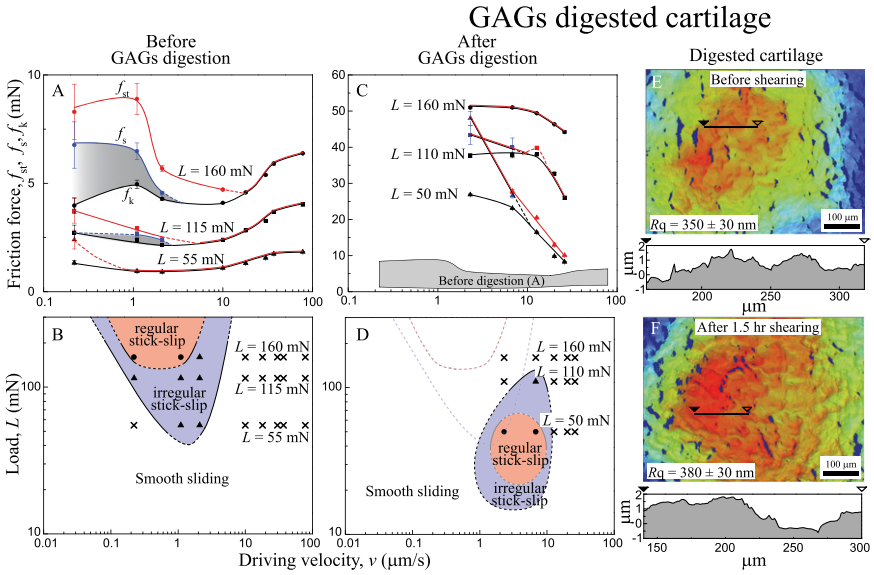

Fig. 4. (*A* and *C*) Friction forces vs. sliding velocity curve and (*B* and *D*) friction maps (*A* and *B*) before and (*C* and *D*) after GAGs digestion. (*E* and *F*) 3D images (top view) of GAGs-digested cartilage (*E*) before and (*F*) after 1.5 h shearing (1 h stick-slip and 0.5 h smooth sliding conditions).

force (up to five times) (Fig. 4*C*), (*ii*) complete disappearance of stick-slip friction in the measurable range of L and v (Fig. 4*D*), (*iii*) disappearance (flattening, $Rq \rightarrow 180 \pm 40$ nm) of the valleys present in healthy cartilage, and (*iv*) significant abrasive wear, which caused further smoothing ($Rq \rightarrow 90 \pm 40$ nm), after 1.5 h of shearing. The fact that the friction force increased as the cartilage surfaces became smoother again indicates that friction forces and surface roughness are not directly correlated.

Generic Friction Map Under Mild Sliding Conditions and Effect of Selective Digestion. Fig. 6*A* shows a generic friction phase diagram of articular cartilage determined from experimental data under mild sliding conditions at varying L and v. With increasing L (blue to red solid lines), a stick-slip sliding regime seems above a certain critical load (L_c). With increasing L above L_c, the stick-slip window, as determined by v_c^I and v_c^{II}, becomes wider, and the magnitude of the stick-slip spikes [$\Delta f = (f_s - f_k)$] (Fig. 6*A*, dashed line) increase. When the driving velocity was initially set below v_c^I and increased to $v > v_c^{II}$ at the fixed load of $L > L_c$, the cartilage goes through three lubrication regimes: (*i*) DBL, (*ii*) transition (also mixed), and (*iii*) FFL.

The DBL regime occurs when $v < v_c^I$. Because of the low velocity, the shearing interface maintains a fluid-like but high-viscosity phase, causing smooth sliding. As v increases and exceeds v_c^I with increasing v, both f_k and thin (DBL) film viscosity fall, giving rise to stick-slip behavior (13, 43). When v exceeds the second critical velocity, v_c^{II}, the cartilage surfaces are separated by a thicker or Newtonian liquid film of fluid. The stick-slip behavior disappears, the surfaces slide smoothly, and f_k now increases with v. When L is lower than L_c, both critical velocities disappear, exhibiting smooth sliding at all velocities.

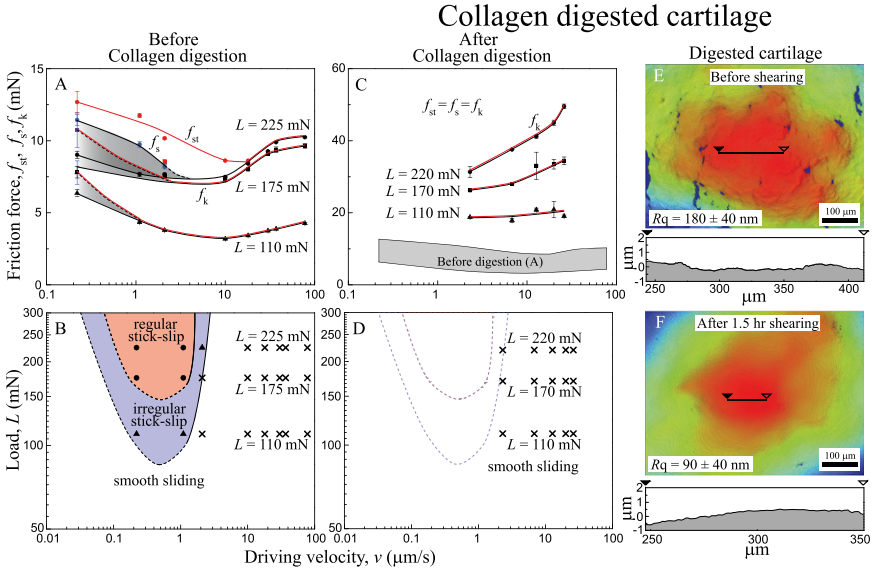

Fig. 5. (*A* and *C*) Friction forces vs. sliding velocity curve and (*B* and *D*) friction maps (*A* and *B*) before and (*C* and *D*) after collagen digestion. (*E* and *F*) 3D images (top view) of collagen-digested cartilage (*E*) before and (*F*) after 1.5 h shearing.

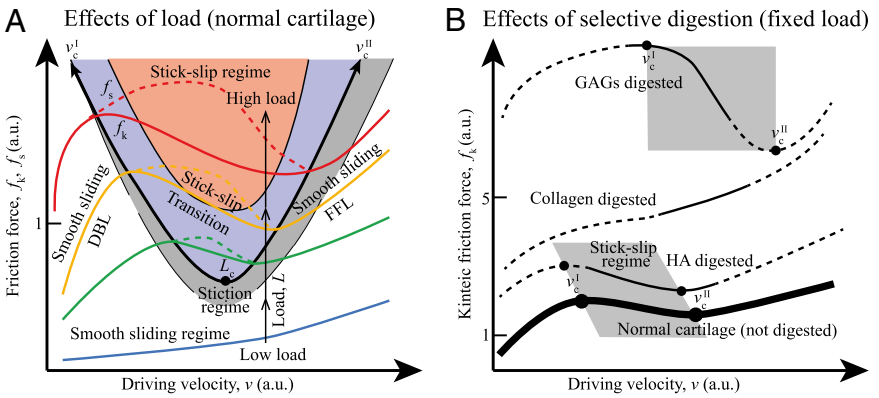

Fig. 6. Generic friction maps of cartilage frictional behavior under mild sliding conditions. (*A*) Effect of load on friction map. Orange, purple, and gray shades indicate regular stick-slip, irregular stick-slip, and stiction regimes, respectively. (*B*) Effect of selective digestions. Dashed lines indicate the extrapolated trends expected from numerous experiments and theories (15). Closed circles indicate critical velocities when stick-slip appears (v_c^I) and disappears (v_c^{II}). Gray shades indicate stick-slip regime windows.

Thus, we conclude that, for cartilage to have stick-slip behavior, the applied load should be higher than L_c, and the driving velocity should be between the two critical velocities, v_c^I and v_c^{II}. We suspect that there will be an upper critical load where cartilage becomes too stiff to exhibit stick-slip behavior (13, 44), although we were not able to reach this point.

Friction experiments with selectively digested cartilage did give us a substantial amount of quantitative and qualitative data regarding the role of the essential components of articular cartilage (Fig. 6*B*). Compared with normal cartilage (Fig. 6*B*, thick solid line), HA digestion has a minimal effect, slightly shifting the generic friction curve to the upper left position (a roughly doubling of the friction force). Collagen and GAGs digestions have a more pronounced effect (up to 5 times higher f_k for collagen-digested cartilage and 10 times higher f_k for GAGs-digested cartilage). Collagen digestion makes stick-slip friction disappear, whereas GAGs digestion shifts the stick-slip regime to higher v.

Molecular Mechanism of Stick-Slip Friction in Articular Cartilage. Fig. 7 presents the schematic of normal and digested cartilage, indicating changes in the interfacial and bulk structure of the superficial zone after digestion that affect the molecular mechanism of stick-slip friction. Normal cartilage exhibits the largest stick-slip amplitude, Δf, compared with selectively digested cartilage (Table 1), possibly because of transient adhesive bridges [caused by transient formation of entanglement, interpenetration, and/or specific polymer–protein interaction, which are dynamically (instead of statically) broken] caused by GAG–GAG (45, 46) interactions and/or entanglements between HA–HA (27). Short-period (~1 h) stick-slip sliding of normal articular cartilage did not generate morphological changes of the cartilage surface. One reason for this finding is that all of the components in normal cartilage work cooperatively (Fig. 7*A*), resulting in a low friction force and excellent wear protection. GAGs-bound HA is effectively trapped in the collagen network, and LUB and lipids collaborate together with immobilized HA for effective lubrication and wear protection at the cartilage interfaces (9). Although the stick-slip peak was relatively larger compared with other digested cartilage, normal cartilage had the lowest f_k (Fig. 6*B*) and the best wear protection property, with no observable morphological changes after shearing for 1.5 h (Table 1).

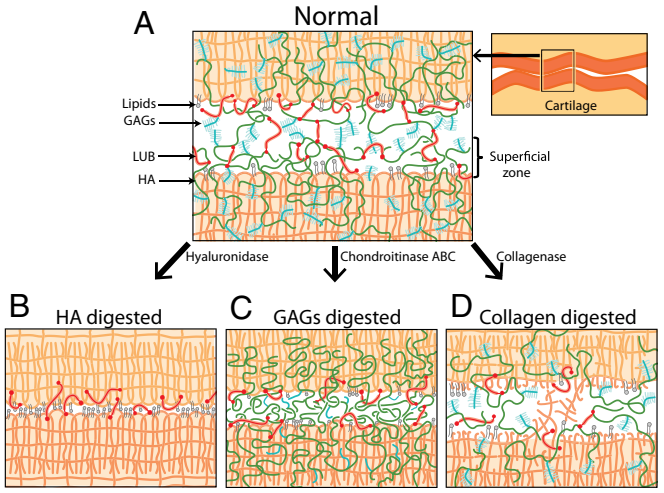

Fig. 7. Schematics of cartilage interfaces indicating molecular mechanism of stick-slip friction (*A*) before and (*B–D*) after selective digestions.

When treated with hyaluronidase, HA chains are cleaved to a shorter molecular mass. Accordingly, the trapping of HA decreases, increasing their probability to diffuse out from the cartilage matrix (9). Furthermore, LUB and lipid molecules that were bound to HA at the cartilage interface can detach more easily together with HA (Fig. 7*B*), leading to direct collagen–collagen contact (which involves hydrophobic forces) (47), which is likely to be the origin of the stick-slip friction for HA-digested cartilage. Direct collagen–collagen contact not only shifts the stick-slip velocity regime but also increases the friction forces and makes cartilage more susceptible to abrasive wear (Fig. 3). We and others (10, 41) have recently found that HA digestion significantly stiffens cartilage, which could have an impact on stick-slip behavior.

GAGs-digested cartilage behaves differently compared with HA-digested cartilage, because cleaving chondroitin sulfate from the GAGs side chains allows the negative charge of GAGs to decrease (Fig. 7*C*). This decrease in negative charge disrupts the osmotic balance between cartilage and the bulk fluid, and the collagen network loses the ability to hold water effectively inside the matrix. Because of the absence of the bulky and highly hydrated GAGs molecules, HA molecules are now more likely to interpenetrate and entangle across the opposing cartilage surfaces, which could be a possible origin of stick-slip in GAGs-digested cartilage.

Unlike hyaluronidase or Case ABC, collagenase dissects the collagen fibers (Fig. 7*D*). The dramatic softening of the collagen

Table 1. Comparison of stick-slip and wear between normal and selectively digested cartilages

	Normalized stick-slip $\Delta f/f_s$	Morphological change after 1.5 h (1 h stick-slip/0.5 h smooth) shearing	Reasons
Normal	High	None*	Interpenetration and effective trapping of the HA Lubricin can bind/bridge both surfaces GAGs–GAGs interaction
HA-digested	Medium	Medium	Less HA trapped in pore structure Less stability of the HA-bound Lubricin Direct collagen–collagen contact
GAGs-digested	Low	Low	Interpenetration/bridging of the HA Lubricin can bind/bridge both surfaces
Collagen-digested	None	High	Deformations and rupture of the collagen fibrils

*When sheared for 10 h under stick-slip conditions, it showed medium change of surface morphology.

matrix allows for large deformations and rupture of the fibrils to occur during sliding, which decreases the ability of the surfaces to form transient adhesive bridges responsible for stick-slip motion (Figs. 5, 6*B*, and 7*D*).

Significance of Stick-Slip Friction in Cartilage. ***Stick-slip motion as the origin of cartilage wear under mild shearing conditions.*** Many excessive sports and workouts put joint health in jeopardy, because joints are exposed to extreme conditions, such as high-impact loads and fast shearing speeds. However, it is surprising that many people also suffer from pain when they simply get up from the bed, sit, or stand still for a long time, both of which are known to be mild conditions for cartilage. These latter symptoms are much more prevalent and significant among arthritic patients, but the primary causes of joint pain under mild conditions are still not well-known. Stick-slip friction is a very common type of friction that is known to lead to abrasive wear (13, 43). We propose that stick-slip friction in articular cartilage may be one—or even the major—cause of wear under mild shearing conditions not only for arthritic cartilage but also, healthy cartilage when sheared for prolonged periods of time.

Damage caused by stick-slip may also occur under more severe conditions. Importantly, we find that the stick-slip amplitude Δf (typically in the range 0–2 mN or 0–2 g) or slip length (typically in the range 10–50 μm) need not be large for damage to occur; this finding may be the reason that this phenomenon has not been previously reported, because most biotribometers measure the average friction force and usually lack the force, time, and distance resolution (sensitivity) of the SFA used in these studies. ***To a noninvasive and cost-effective diagnostic tool for arthritis.*** In the United States, over 50 million adults suffer from arthritis, and the numbers are growing rapidly. Conventional diagnostic tools for arthritis are often invasive (e.g., synovial fluid test and blood test) and/or costly (e.g., X-ray and MRI), and the demand for noninvasive and cost-effective diagnostic tools for arthritis is increasing. Although these clinical in vivo tests should, of course, be performed, our results indicate that more sensitive friction tests should be implemented that could identify early stages of cartilage degeneration. Stick-slip friction can be recorded by the sound that it generates (compare with the sound from a violin, the squeaking noise of a door, the noise from a breaking car, etc.) (43). An acoustic device could easily detect and systematically analyze the stick-slip characteristics (frequency and amplitude) of a patient and could be extremely useful as a cost-effective and noninvasive screening tool for arthritis before or in conjunction with other routine diagnoses and treatments.

Materials and Methods

Cartilage Sample Preparation. Porcine leg was purchased from Sierra for Medical Science, and cartilage tissue was dissected from porcine knee articular joints no later than 1 d after slaughter. Dissection was performed under room temperature in a laminar hood to minimize contamination. During dissection, cartilage samples were kept in a wet condition by continuous rinsing with HBSS. Full-thickness (~3 mm, from the superficial zone down to the calcified zone) cartilage was dissected with a razor blade and stored in Hanks' solution at −50 °C until use (storage duration was at most 1 mo). Two flat glass disks were cleaned using chloroform followed by ethanol before use. The flat sides of the cartilage samples were partially dried using lint-free cloth and then glued onto glass disks using poly(cyanoacrylate) adhesive followed by curing in PBS buffer for 30 min.

SFA Experiment. Glued cartilage surfaces were mounted to an SFA2000 equipped with a friction device or a 3D sensor/actuator with bimorph slider (48). In this study, an SFA2000 is used as a microtribometer (49) with high resolution in measuring both load and friction (up to ~0.01 mN). The SFA chamber was saturated with water vapor to minimize evaporation of water in cartilage. Between the two facing cartilage surfaces, 200 μL equine synovial fluid (Alamo Pintato) for the experiment in Fig. 2 *C* and *D* or PBS (Sigma) for all other experiments were injected as a reservoir. Loading and shearing were conducted with course-control micrometer and bimorph slider, respectively, whereas the friction forces and loads were measured using a recently developed 3D sensor/actuator (48, 50). Because of the opacity of the samples, optical interferometry could not be used as in standard SFA-Fringes of Equal Chromatic Order (FECO) experiments. Although the cartilage surfaces were being compressed under a constant load, they were sheared laterally at a fixed driving velocity ranging from 0.03 to 100 μm/s with sliding a amplitude of ~100 μm until the measured loads and friction forces reached the steady state (Fig. 1*B*). After measuring friction forces at a wide range of driving velocities, the load was varied, and friction forces were again measured. Measurements were repeated for three to four different loads. After SFA experiment with normal cartilage, 50 μL enzyme for selective digestion (hyaluronidase, 200 units/mg in PBS; Sigma), type II collagenase (2,000 units/mg in PBS; Sigma), and Case ABC (137 units/mg in PBS; Sigma) were injected between the surfaces and equilibrated for 3 h. After digestion, surfaces were rinsed with PBS buffer. The SFA experiments were then repeated with digested cartilage using the same procedure as mentioned above.

Interferometric Imaging. A Wyko 1100 white-light interferometer (Veeco) was used to image surface topography of the cartilage. Right before mounting the sample on the stage, the cartilage surface was briefly dried with nitrogen under a laminar flow hood to minimize abnormal signals generated by water reflection. Cartilage position was carefully adjusted to the center of the stage to image the highest point, which is actually being sheared in the SFA experiments. The rms roughness *R*q was calculated by averaging fiv random windows (80 × 80 μm) after tilt and curvature fitting using Vision32 software.

Glued cartilage surfaces were digested with each enzyme and imaged with a Wyko 1100 white-light interferometer before shearing to characterize the effects of digestions. After imaging, they were sheared for 1.5 h (1 h under stick-slip sliding and 0.5 h under smooth sliding) and imaged again to in-

vestigate the effects of the shearing. For normal (nontreated) cartilage, imaging was performed under the same procedure; however, because it did not show any change in roughness after 1.5 h of shearing, 10 h of shearing under stick-slip condition were performed to see the effects of prolonged stick-slip shearing on healthy cartilage.

ACKNOWLEDGMENTS. We thank Alamo Pintado Equine Medical Center for supplying us with equine synovial fluid. We also thank Drs. David Bothman and Kimberly Turner for access to the Wyko Interferometer. X.B. would like to thank the Otis Williams Fellowship for their support. This work was funded by McCutchen Foundation.

1. McAlindon TE, Wilson PWF, Aliabadi P, Weissman B, Felson DT (1999) Level of physical activity and the risk of radiographic and symptomatic knee osteoarthritis in the elderly: The Framingham study. *Am J Med* 106(2):151–157.
2. Felson DT, et al. (2000) Osteoarthritis: New insights. Part 1: The disease and its risk factors. *Ann Intern Med* 133(8):635–646.
3. Grotle M, Hagen KB, Natvig B, Dahl FA, Kvien TK (2008) Obesity and osteoarthritis in knee, hip and/or hand: An epidemiological study in the general population with 10 years follow-up. *BMC Musculoskelet Disord* 9:5.
4. Loeser RF (2006) Molecular mechanisms of cartilage destruction: Mechanics, inflammatory mediators, and aging collide. *Arthritis Rheum* 54(5):1357–1360.
5. Schouten JS, van den Ouweland FA, Valkenburg HA (1992) A 12 year follow up study in the general population on prognostic factors of cartilage loss in osteoarthritis of the knee. *Ann Rheum Dis* 51(8):932–937.
6. Katta J, Jin ZM, Ingham E, Fisher J (2008) Biotribology of articular cartilage—a review of the recent advances. *Med Eng Phys* 30(10):1349–1363.
7. Forster H, Fisher J (1996) The influence of loading time and lubricant on the friction of articular cartilage. *Proc Inst Mech Eng H* 210(2):109–119.
8. Forster H (1996) *Mixed and Boundary Lubrication in Natural Synovial Joints. Doctor of Philosophy* (University of Leeds, Leeds, United Kingdom).
9. Greene GW, et al. (2011) Adaptive mechanically controlled lubrication mechanism found in articular joints. *Proc Natl Acad Sci USA* 108(13):5255–5259.
10. Greene GW, et al. (2012) Hyaluronic acid–collagen network interactions during the dynamic compression and recovery of cartilage. *Soft Matter* 8(38):9906–9914.
11. Guilak F, Ratcliffe A, Lane N, Rosenwasser MP, Mow VC (1994) Mechanical and biochemical changes in the superficial zone of articular cartilage in canine experimental osteoarthritis. *J Orthop Res* 12(4):474–484.
12. Ateshian GA (2009) The role of interstitial fluid pressurization in articular cartilage lubrication. *J Biomech* 42(9):1163–1176.
13. Berman AD, Ducker WA, Israelachvili JN (1996) Origin and characterization of different stick-slip friction mechanisms. *Langmuir* 12(19):4559–4563.
14. Israelachvili JN (2010) *Intermolecular and Surface Forces* (Academic and Elsevier, Amsterdam), 3rd Ed.
15. Drummond C, Israelachvili J, Richetti P (2003) Friction between two weakly adhering boundary lubricated surfaces in water. *Phys Rev E Stat Nonlin Soft Matter Phys* 67(6 Pt 2):066110.
16. Balazs EA, Watson D, Duff IF, Roseman S (1967) Hyaluronic acid in synovial fluid. I. Molecular parameters of hyaluronic acid in normal and arthritis human fluids. *Arthritis Rheum* 10(4):357–376.
17. Dahl LB, Dahl IMS, Engström-Laurent A, Granath K (1985) Concentration and molecular weight of sodium hyaluronate in synovial fluid from patients with rheumatoid arthritis and other arthropathies. *Ann Rheum Dis* 44(12):817–822.
18. Holmes MWA, Bayliss MT, Muir H (1988) Hyaluronic acid in human articular cartilage. Age-related changes in content and size. *Biochem J* 250(2):435–441.
19. Nagase H, Kashiwagi M (2003) Aggrecanases and cartilage matrix degradation. *Arthritis Res Ther* 5(2):94–103.
20. Aigner T, Kurz B, Fukui N, Sandell L (2002) Roles of chondrocytes in the pathogenesis of osteoarthritis. *Curr Opin Rheumatol* 14(5):578–584.
21. Sandell LJ, Aigner T (2001) Articular cartilage and changes in arthritis. An introduction: Cell biology of osteoarthritis. *Arthritis Res* 3(2):107–113.
22. McCutchen CW (1966) Boundary lubrication by synovial fluid—demonstration and possible osmotic explanation. *Fed Proc* 25(3P1):1061–1068.
23. McCutchen CW (1966) Physiological lubrication. *Proc Inst Mech Eng* 181(Pt3J):55–62.
24. Graindorge S, et al. (2006) The role of the surface amorphous layer of articular cartilage in joint lubrication. *Proc Inst Mech Eng H* 220(5):597–607.
25. Swann DA, et al. (1974) Role of hyaluronic acid in joint lubrication. *Ann Rheum Dis* 33(4):318–326.
26. Benz M, Chen NH, Israelachvili J (2004) Lubrication and wear properties of grafted polyelectrolytes, hyaluronan and hylan, measured in the surface forces apparatus. *J Biomed Mater Res A* 71(1):6–15.
27. Yu J, Banquy X, Greene GW, Lowrey DD, Israelachvili JN (2012) The boundary lubrication of chemically grafted and cross-linked hyaluronic acid in phosphate buffered saline and lipid solutions measured by the surface forces apparatus. *Langmuir* 28(4):2244–2250.
28. Ford IJ (1993) Roughness effect on friction for multi-asperity contact between surfaces. *J Phys D Appl Phys* 26(12):2219–2225.
29. Quaglini V, Dubini P, Ferroni D, Poggi C (2009) Influence of counterface roughness on friction properties of engineering plastics for bearing applications. *Mater Des* 30(5): 1650–1658.
30. Muir H (1995) The chondrocyte, architect of cartilage. Biomechanics, structure, function and molecular biology of cartilage matrix macromolecules. *Bioessays* 17(12): 1039–1048.
31. Kampf N, Raviv U, Klein J (2004) Normal and shear forces between adsorbed and gelled layers of chitosan, a naturally occurring cationic polyelectrolyte. *Macromolecules* 37(3):1134–1142.
32. Raviv U, et al. (2003) Lubrication by charged polymers. *Nature* 425(6954):163–165.
33. Lee S, Spencer ND (2008) Materials science. Sweet, hairy, soft, and slippery. *Science* 319(5863):575–576.
34. Basalo IM, Chen FH, Hung CT, Ateshian GA (2006) Frictional response of bovine articular cartilage under creep loading following proteoglycan digestion with chondroitinase ABC. *J Biomech Eng* 128(1):131–134.
35. Maeda N, Chen NH, Tirrell M, Israelachvili JN (2002) Adhesion and friction mechanisms of polymer-on-polymer surfaces. *Science* 297(5580):379–382.
36. ap Gwynn I, Wade S, Ito K, Richards RG (2002) Novel aspects to the structure of rabbit articular cartilage. *Eur Cell Mat* 4(Dec. 10):18–29.
37. Eyre D (2002) Collagen of articular cartilage. *Arthritis Res* 4(1):30–35.
38. Greene GW, et al. (2010) Anisotropic dynamic changes in the pore network structure, fluid diffusion and fluid flow in articular cartilage under compression. *Biomaterials* 31(12):3117–3128.
39. Greene GW, et al. (2008) Changes in pore morphology and fluid transport in compressed articular cartilage and the implications for joint lubrication. *Biomaterials* 29(33):4455–4462.
40. Lewis PR, McCutchen CW (1959) Experimental evidence for weeping lubrication in mammalian joints. *Nature* 184(4695):1285–1285.
41. Stolz M, et al. (2009) Early detection of aging cartilage and osteoarthritis in mice and patient samples using atomic force microscopy. *Nat Nanotechnol* 4(3):186–192.
42. Venn M, Maroudas A (1977) Chemical composition and swelling of normal and osteoarthrotic femoral head cartilage. I. Chemical composition. *Ann Rheum Dis* 36(2): 121–129.
43. Yoshizawa H, Israelachvili J (1993) Fundamental mechanisms of interfacial friction. 2. Stick-slip friction of spherical and chain molecules. *J Phys Chem* 97(43):11300–11313.
44. Rabinowicz E (1966) *Friction and Wear of Materials* (Wiley, New York), 2nd Ed.
45. Han L, Dean D, Daher LA, Grodzinsky AJ, Ortiz C (2008) Cartilage aggrecan can undergo self-adhesion. *Biophys J* 95(10):4862–4870.
46. Han L, Grodzinsky AJ, Ortiz C (2011) Nanomechanics of the cartilage extracellular matrix. *Annual Review of Materials Research, Vol 41,* Annual Review of Materials Research, eds Clarke DR, Fratzl P (Annual Reviews, Palo Alto, CA), Vol 41, pp 133–168.
47. Wallace D (1985) The role of hydrophobic bonding in collagen fibril formation: A quantitative model. *Biopolymers* 24(9):1705–1720.
48. Israelachvili J, et al. (2010) Recent advances in the surface forces apparatus (SFA) technique. *Rep Prog Phys* 73(3):036601.
49. Yu J, et al. (2011) Gecko-inspired dry adhesive for robotic applications. *Adv Funct Mater* 21(16):3010–3018.
50. Kristiansen K, et al. (2012) Measurements of anisotropic (off-axis) friction-induced motion. *Adv Mater (Deerfield Beach Fla)* 24(38):5236–5241.